Chinese Journal of
POLYMER SCIENCE

RESEARCH ARTICLE

https://doi.org/10.1007/s10118-026-3728-0
Chinese J. Polym. Sci.

Molecularly Engineered Eco-friendly Smart Fabrics with Photoswitchable Wettability: from Highly Hydrophobic to Superhydrophilic

Yi-Ran Wang, Bo-Lun Feng, Hong-Fei Jiang, Lin Zhang, Bin Chen, Hao-Kai Yuan, Lu Wang, and Chuan-Yong Zong*

School of Chemistry and Chemical Engineering, Shandong Provincial Key Laboratory of Extreme Environment-tolerant Specialty Chemicals, University of Jinan, Jinan 250022, China

Electronic Supplementary Information

Abstract Bioinspired smart surfaces enable reversible regulation of surface wettability, which is increasingly important for the advancement of surface and interface science. Herein, a novel fluorine-free photoresponsive azo-copolymer was rationally designed and synthesized *via* a molecular engineering strategy involving the synergistic integration of photoresponsive azobenzene moieties and low-surface-energy organosilicon segments. A facile solution dip-coating method was employed to construct photoresponsive smart fabric surfaces. Benefiting from the excellent reversible trans-cis isomerization of the azobenzene moieties within the azo-copolymer, the resulting coating achieved a notable surface energy variation of up to 32.75 $mN{\cdot}m^{-1}$. The as-prepared smart fabrics exhibited rapid, reversible wettability switching between high hydrophobicity (water contact angle of about 135°) and superhydrophilicity (0°) within 120 s under alternating UV and visible light irradiation. Meanwhile, the smart fabric surfaces exhibited outstanding chemical and mechanical robustness, enabling resistance to harsh environmental conditions, repeated abrasion tests, and various mechanical deformations, such as stretching, curling, and folding. More importantly, as a proof-of-concept demonstration, diverse rewritable wettability patterns were conveniently fabricated on a smart fabric surface *via* selective light exposure. This simple and effective strategy, together with the as-developed smart surfaces, holds great promise for application in information storage, biosensors, and microreactors.

Keywords Azo-copolymer; Smart fabrics; Photoswitchable wettability; Patterned surface; Fluorine-free

Citation: Wang, Y. R.; Feng, B. L.; Jiang, H. F.; Zhang, L.; Chen, B.; Yuan, H. K.; Wang, L.; Zong, C. Y. Molecularly engineered eco-friendly smart fabrics with photoswitchable wettability: from highly hydrophobic to superhydrophilic. *Chinese J. Polym. Sci.* https://doi.org/10.1007/s10118-026-3728-0

INTRODUCTION

Stimuli-responsive material surfaces, which can dynamically tailor their structures and/or physicochemical properties in response to external stimuli, are of fundamental and technological importance in materials science.[1–3] Among them, smart superwetting surfaces featuring reversibly tunable wettability have been rationally engineered for diverse promising applications, such as controllable liquid transport,[3,4] functional coatings,[5,6] sensors,[7] biomedical engineering,[8] oil-water separation,[9,10] and others.[2,11] Recent advances have demonstrated that the rational control of surface microstructures and/or fine-tuning of surface chemistry constitute an effective strategy for programming smart superwetting surfaces.[3,12,13] For instance, by constructing spherical polyurethane-mushroom structured shape-memory epoxy resin arrays on Fe_3O_4-doped substrates, a photo/thermo-responsive material with reversibly switchable solid/liquid adhesion, excellent cycling stability, and universal applicability was developed for the selective capture of silicon wafers and water droplets *via* reversible structural transformation.[14] Integrating carbonyl iron particles (CIP) into a shape-memory polymer fabricates a near-infrared light-responsive photothermal pillar array, where the bent microstructured surface exhibits high water adhesion (98 μN), whereas the recovered micro/nanostructured surface shows low adhesion (25 μN) and an ultralow rolling-off angle of 4°.[15] A bioinspired intelligent surface constructed from CIP-incorporated thermoresponsive shape-memory polyurethane composites with high-aspect-ratio columnar micropillars exhibited photo/thermal/magnetic triple-stimulus responsiveness and robust cross-species wetting regulation under coupled stimuli, highlighting its potential as a scalable, programmable interfacial platform.[16] However, the sophisticated fabrication and equipment dependence of microarray structures restrict their practical applications. In contrast, integrating stimuli-responsive moieties to tailor the surface chemistry affords a facile, universal strategy for smart su-

* Corresponding author, E-mail: chm_zongcy@ujn.edu.cn
Received April 9, 2026; Accepted April 25, 2026; Published online July 6, 2026

perwetting surfaces. Currently, diverse stimuli-responsive materials toward temperature,[4,17] voltage,[18] magnetic fields,[19,20] light,[5,21] and pH,[22,23] afford tailored options for the rational design and fabrication of smart superwetting surfaces. Moreover, light serves as a clean external stimulus that can be remotely controlled with a high spatiotemporal resolution and rapid response, thereby attracting substantial attention to photoresponsive materials for regulating surface wettability switching. To date, various inorganic photosensitive materials such as titanium dioxide,[24,25] zinc oxide,[26] and vanadium oxide,[27] as well as typical organic photoresponsive molecules such as azobenzene,[28,29] and spiropyran,[30,31] have been widely utilized as photoresponsive building blocks to fabricate smart superwetting surfaces for applications in oil-water separation, droplet manipulation, and information storage. The prominent photoisomerization of azobenzene derivatives, accompanied by a distinct molecular dipole moment variation, endows the corresponding superwetting surfaces with rapid and pronounced wettability switching.[3,32] Thus far, numerous research efforts have been devoted to constructing photoresponsive superwetting surfaces *via* strategies such as grafting of small azobenzene molecules and coating of azobenzene-based polymers. For instance, an azobenzene-based metal-organic framework nanoporous film achieved wide-range wettability tuning from 23° to 97° *via* photoswitching of fluorinated azobenzene moieties and the reversible insertion of guest molecules.[33] By incorporating a photoisomerizable azobenzene-based molecular motor into the surface liquid layer, UV irradiation generates an isomerization gradient that drives fluid flow, forming a light-driven liquid conveyor capable of transporting both water droplets and microsolids.[34] Novel azobenzene-modified fluorinated epoxy-isocyanate networks enable controllable coating hydrophobicity *via trans-cis* isomerization-driven changes in the surface polarity and roughness.[35] In our previous study, various fluorinated azobenzene-containing copolymers were synthesized and deposited onto porous substrates to construct light-responsive superwetting surfaces, enabling rapid and reversible hydrophobic-to-hydrophilic switching.[5,28,36] Notably, the incorporation of fluorinated moieties can significantly enhance the intrinsic hydrophobicity and coating stability of superwetting surfaces. Nevertheless, growing environmental concerns regarding fluorinated chains have spurred the development of fluorine-free, greener photoresponsive polymers for the fabrication of smart superwetting surfaces.

In this work, a novel fluorine-free photoresponsive azo-copolymer was designed and synthesized by employing low-surface-energy organosilicon moieties instead of controversial fluorine-containing segments, in line with the principles of green chemistry. The chemical structure of the azo-copolymer and the photo-triggered trans-cis isomerization kinetics of the azobenzene moieties within the azo-copolymer were systematically characterized by nuclear magnetic resonance (NMR), Fourier transform infrared (FTIR) spectroscopy and ultraviolet-visible (UV-Vis) spectroscopy. A cotton fabric-based smart surface was then fabricated *via* a simple dip-coating approach using an azo-copolymer solution, which enabled reversible photoswitching of the surface wettability between high hydrophobicity and superhydrophilicity. The reversible photoswitchable wettability of the smart fabric surface and its underlying mechanism, as well as the chemical resistance to acidic/alkaline corrosion and mechanical robustness of the azo-copolymer coating on the fabric, were systematically explored. More importantly, as a proof-of-concept application, diverse rewritable patterns with distinct wettability can be conveniently constructed on smart fabric surfaces through selective light exposure. Such intelligent superwettable surfaces show promising application potential for directional droplet transport, patterned droplet microarrays, and information storage.

EXPERIMENTAL

Materials

Tetrahydrofuran (THF) and *N*,*N*-dimethylformamide (DMF) were purchased from Fuyu Fine Chemical Co. Ltd. (Tianjin, China). 2,2-Azobisisobutyronitrile (AIBN) was obtained from Laiyang Kangde Chemical Co., Ltd. (Shandong, China). The azobenzene monomer (Azo) was synthesized in our laboratory according to our previous work.[5,28] Methacrylate siloxane oligomer (MPTSS) was purchased from Sinuoke Organosilicon Co., Ltd. Cotton fabrics were purchased from Weifang Qianjia Textile Co., Ltd. (Weifang, China). All other reagents were of analytical grade and used as received without further purification.

Synthesis of Azo-copolymers Poly(Azo-*co*-MPTSS)

Photoresponsive poly(Azo-*co*-MPTSS) was synthesized by free-radical solution polymerization. Briefly, Azo, MPTSS, and AIBN were dissolved in DMF, and the mixture was polymerized at 75 °C for 24 h under nitrogen protection. After cooling to room temperature, the reaction solution was added dropwise to deionized water. The resulting precipitate was purified by three repeated dissolution-precipitation cycles in DMF and deionized water, followed by vacuum drying to yield the final yellow solid powder. Unless stated otherwise, poly(Azo-*co*-MPTSS) with an Azo:MPTSS molar ratio of 8:1 was used in this study.

Fabrication of Cotton Fabric-based Smart Surfaces

White cotton fabric (2 cm × 2 cm squares) was cleaned by ultrasonication in ethanol and acetone for 30 min successively and dried at 50 °C. Subsequently, the dried fabric was fully immersed in a 5 wt% poly(Azo-*co*-MPTSS)/THF solution, sonicated for 30 min, and dried.

Characterization

^{1}H-NMR spectra of the azo-monomer and azo-copolymer were recorded on an Advance III 400 MHz NMR spectrometer (Bruker, Germany) using deuterated DMSO as the solvent and tetramethylsilane as the internal standard. FTIR spectra were obtained on a Nicolet Is10 FTIR spectrophotometer (Thermo Fisher, USA) in the range of 500–4000 cm^{-1}, using KBr as the substrate. UV-Vis absorption spectra were recorded on a TU-1901 spectrophotometer. Gel permeation chromatography (Agilent 1100, Dalian Elite, China) was employed to characterize the molecular weight and dispersity ($Đ$) of the azo-copolymer, using THF as thee eluent. Thermogravimetric analysis (TGA) was performed on a Setline STA analyzer over 50–800 °C at 10 °C·min^{-1} under N_2 atmosphere. Differential scanning calorimetry (DSC) was carried out on a Setline DSC calorimeter from 50 °C to 300 °C at 10 °C·min^{-1} under a N_2 atmosphere. The surface morphology and elemental distribution of the samples were investigated using a

Gemini 300 scanning electron microscope (SEM; Zeiss, Germany). The water contact angle (WCA) on the sample surface was characterized by JC2000D6M WCA measurement (Powereach, China) with water droplets of 4 μL. The abrasion durability of the coating was evaluated by reciprocating friction tests on modified fabrics using 1000 CW sandpaper under a constant load of 20 g for 20 cycles. For the photo-regulated surface wettability tests, the UV light source was set at λ=365 nm with a light intensity of 34.6 mW·cm^{-2}, while the visible light source was λ=450 nm with a light intensity of 266 mW·cm^{-2}.

RESULTS AND DISCUSSION

Side-chain-functionalized azo-containing copolymers were synthesized *via* solution free-radical polymerization by synergistically integrating the photoresponsive azobenzene and low-surface-energy organosilicon moieties (Fig. 1a). Specifically, long alkyl spacers tethered to azobenzene moieties improve both chain mobility and hydrophobicity, whereas long-chain organosilicon segments endow the copolymer with outstanding low-surface-energy characteristics. As illustrated in Fig. 1(b), a smart cotton fabric with phototunable surface wettability was fabricated *via* a facile dip-coating process. Reversible photoisomerization of the azobenzene moieties in the side chains induces dynamic variations in surface energy, thereby imparting a coated fabric with reversible light-switchable surface wettability. Notably, the *trans-cis* photoisomerization of azobenzene moieties is generally accompanied by macroscopic color variations in azo-polymers. As shown in Fig. S1 (in the electronic supplementary information, ESI), the as-synthesized poly((Azo-*co*-MPTSS) changed from light yellow to orange yellow under UV irradiation and reverted to its original color upon visible-light irradiation. This reversible photochromism directly confirms the successful photoisomerization of the azobenzene moieties in the azo-copolymer. The chemical structures of the azo-copolymers with different comonomer molar ratios were characterized using ^{1}H-NMR and FTIR spectroscopy (Figs. 1c and 1d). As demonstrated in Fig. 1(c), the characteristic peaks at 6.90–7.95 ppm are assigned to the aromatic —CH— groups of the benzene rings.[28] The characteristic peak at 4.15 ppm corresponds to —CH_2— moieties in the azo-copolymer side chains. The signals at 1.20–1.80 ppm are attributed to the —CH_3 and —CH_2— groups in the main chain.[37] FTIR analysis further verified the chemical structure of the azo-copolymers (Fig. 1d). The characteristic stretching bands of —CH_3 and —CH_2— appear at 2940 and 2869 cm^{-1}, respectively[5]. A strong C=O stretching vibration was observed at 1730 cm^{-1}, together with aromatic skeletal vibrations of benzene rings at 1615 cm^{-1} and Si—O—Si absorp-

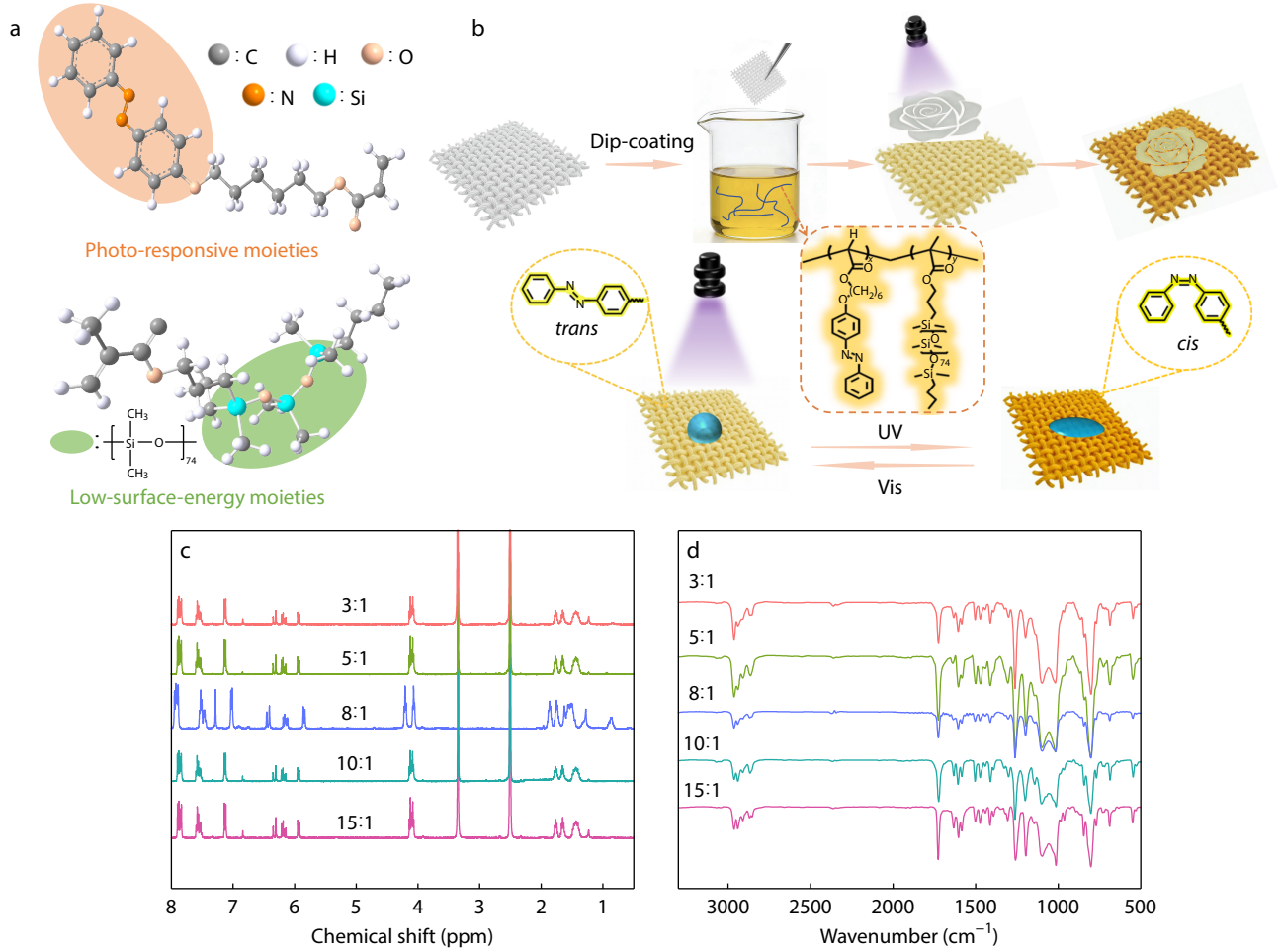

Fig. 1 (a) Molecular structures of functional monomers and (b) schematic illustration of the fabrication procedure for cotton fabric-based smart surfaces *via* dip-coating; (c) ^{1}H-NMR and (d) FTIR spectra of the as-synthesized poly(Azo-*co*-MPTSS) with different Azo:MPTSS molar ratios.

https://doi.org/10.1007/s10118-026-3728-0

tions at approximately 1000 cm^{-1}.[38] Notably, no obvious peaks were detected in the region 1640–1680 cm^{-1}, characteristic of C=C double bonds, indicating full consumption of the monomers during polymerization.[37] These results collectively confirmed the successful synthesis of poly(Azo-*co*-MPTSS). The number-average molecular weight (M_n) and $Đ$ of the as-synthesized poly(Azo-*co*-MPTSS) copolymer are 2.9×10^3 and 1.46, respectively (Fig. S2 and Table S1 in ESI). Moreover, the copolymer exhibited a glass transition temperature (T_g) of 54.82 °C and a 5 wt% thermal decomposition temperature ($T_{d5\%}$) of 236.27 °C, demonstrating excellent thermal stability (Fig. S3 in ESI).

As a representative photoresponsive chromophore, azobenzene and its derivatives feature a stable *trans*- and metastable *cis* isomer that can be reversibly interconverted under light irradiation at appropriate wavelengths.[39,40] Similar to other azobenzene-containing polymers, the as-synthesized azo-copolymer exhibited excellent photoresponsive behavior in THF solution owing to the *trans-cis* isomerization of the azobenzene moieties. As shown in Figs. 2(a) and 2(b), the UV-Vis absorption spectrum of the azo-copolymer displays characteristic bands at approximately 350 and 440 nm, corresponding to the π-π^* and n-π^* electronic transitions of azobenzene, respectively.[36,41] Upon UV irradiation, the π-π^* absorption at 350 nm decreased rapidly and blue-shifted to 304 nm within 10 s, accompanied by a gradual increase in the n-π^* absorption near 450 nm, indicating photoisomerization

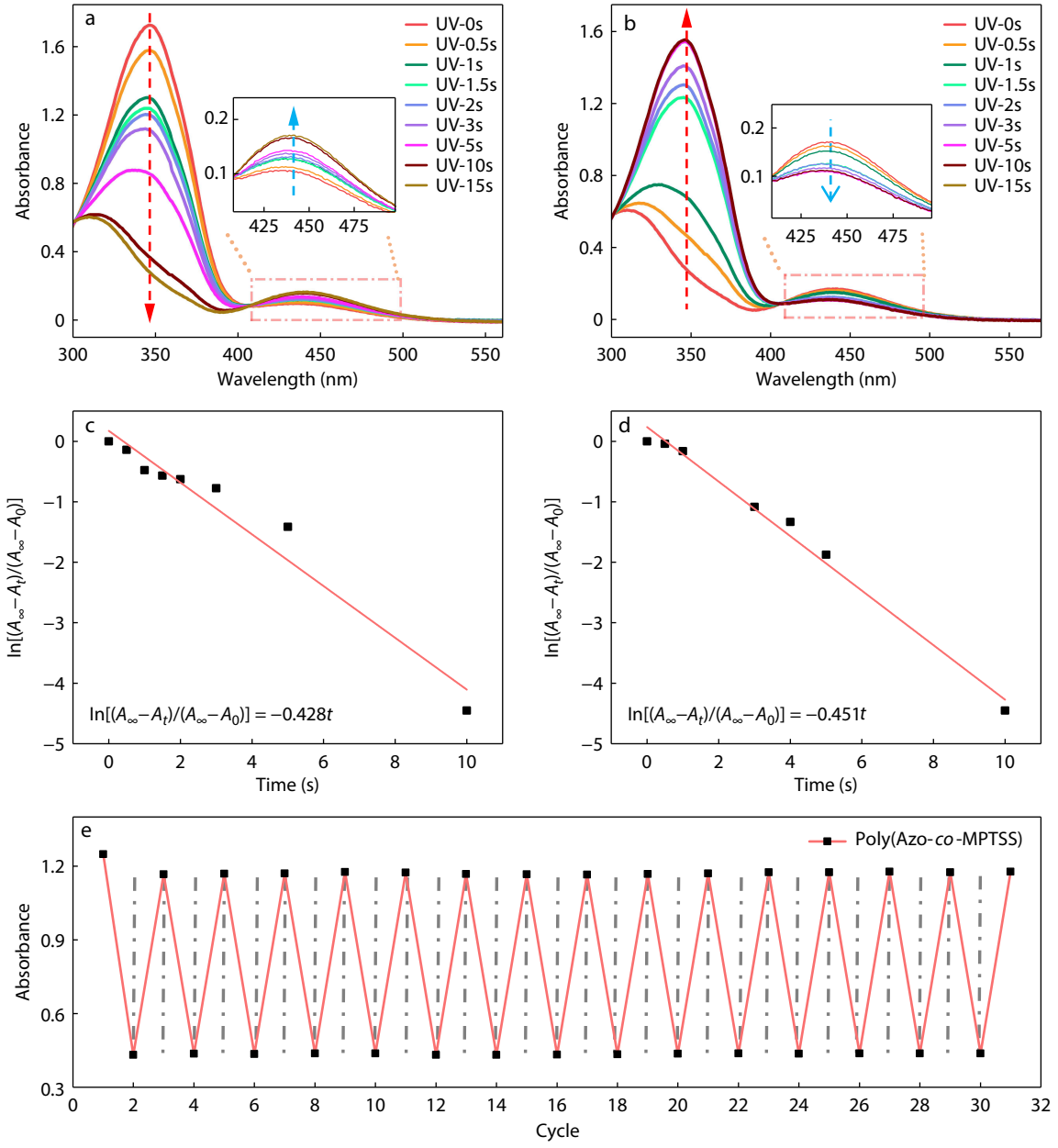

Fig. 2 UV-Vis absorption spectra of poly(Azo-*co*-MPTSS) solution (0.003 wt%) under (a) 365 nm UV irradiation and (b) 450 nm visible-light irradiation; Kinetic fitting of *trans-cis* (c) and *cis-trans* (d) isomerization in CH_2Cl_2 solution (red lines: simulated curves; black dots: experimental data); (e) Absorbance variations at 350 nm of poly(Azo-*co*-MPTSS) solution under alternating UV/Vis light irradiation.

https://doi.org/10.1007/s10118-026-3728-0

from a trans-enriched to *cis*-enriched state (Fig. 2a). Subsequent visible-light irradiation led to gradual recovery of the π-π^* absorption band and a decline in the n-π^* intensity, confirming the reversible photoisomerization back to the initial trans state (Fig. 2b). It is well established that *trans*- and *cis*-azobenzene exhibit a pronounced difference in dipole moment (*trans*: 0.5 D; *cis*: 3.1 D), and an increased dipole moment gives rise to higher surface polarity and thus enhanced wettability toward water droplets.[5,42] Accordingly, the reversible *trans-cis-trans* isomerization cycle of azobenzene moieties endows the poly(Azo-*co*-MPTSS) coating with photo-switchable surface wettability (for a detailed discussion, see the following section). To quantify the azobenzene isomerization kinetics of poly(Azo-*co*-MPTSS) in solution under UV and visible-light irradiation, the first-order rate constant k_{tc} was derived using the following equation:[5,43]

$$\ln\frac{A_\infty - A_t}{A - A_0} = -k_{tc}t \quad (1)$$

where A_0, A_∞, and A_t represent the absorbance values before irradiation, in the photostationary state, and at various irradiation times (t), respectively. The rate constants k_{tc} for UV-induced *trans-cis* and visible-light-triggered *cis-trans* isomerization of azobenzene in the azo-copolymer were determined to be 0.428 and 0.451 s^{-1}, respectively, consistent with those reported for azo-copolymer systems (Figs. 2c and 2d).[36,43] Compared with previously reported azobenzene copolymer systems, the relatively fast photoisomerization rate of the prepared copolymer originates from the flexible long alkyl spacers grafted on azobenzene groups, which effectively reduce steric hindrance and accelerate molecular conformational rearrangement during *trans-cis* structural transformation. Meanwhile, the low-surface-energy silicone segments hardly interfere with the light-induced dipole variation process of the azo groups, thus maintaining efficient and rapid photoisomerization dynamic performance. Moreover, the absorbance of the azo-copolymer solution at 350 nm showed no obvious decay during repeated UV/visible light cyclic irradiation, confirming the excellent photoresponsive stability of the as-synthesized poly(Azo-*co*-MPTSS) (Fig. 2e).

Benefiting from the excellent photoresponsive behavior of the as-synthesized azo-copolymer, a smart fabric surface was constructed on porous cotton fabric substrates *via* a simple dip-coating strategy. SEM characterization showed that the pristine cotton fibers had a relatively smooth surface (Fig. 3a and Fig. S4a in ESI). After modification with poly(Azo-*co*-MPTSS), a conspicuously rough coating layer was observed on the surface (Fig. 3b and Fig. S4b in ESI). Furthermore, SEM-EDS elemental mapping confirmed the uniform distribution of Si, N, C, and O on the modified fabric surface (Figs. 3c and 3d, Figs. S4c and S4d in ESI). The Si signal originates from the organosilicon moieties in the azo-copolymer, whereas the N signal was assigned to the azobenzene moieties, verifying the uniform deposition of poly(Azo-*co*-MPTSS) on the cotton fibers. As anticipated, the organosilicon moieties in the azo-copolymer chains imparted low surface energy and high hydrophobicity to the modified fabric, yielding a static water contact angle (WCA) of approximately 135° (Fig. 3e and Fig. S5 in ESI). Surface energy calculations of the modified fabric showed that the surface energy gradually decreased from 49.00 $mN{\cdot}m^{-1}$ to 42.63 $mN{\cdot}m^{-1}$ with increasing content of organosilicon moieties in the copolymer chains (Fig. S6 and Table S2 in ESI).[44] The WCA remained nearly constant for 120 s under ambient conditions, indicating a robust hydrophobic stability. Meanwhile, the azobenzene moieties endowed the modified fabric with light-responsive surface-wettability switching. Upon UV irradiation, the *trans*-to-*cis* isomerization of azobenzene increases the molecular polarity and induces chain rearrangement, progressively enhancing the surface hydrophilicity and decreasing the WCA.[5] After 20 s of UV irradiation, the fabric surface rapidly changed from highly hydrophobic to superhydrophilic, with a WCA of 0°. Meanwhile, the surface energy of fabrics modified with different azo-copolymers increased to 74.98–75.44 $mN{\cdot}m^{-1}$, respectively (Fig. S6 and Table S2 in ESI). Subsequent visible light irradiation triggered *cis*-to-*trans* recovery, accompanied by a decreased dipole moment and restored hydrophobicity.[36] Within 5 s of visible light irradiation, the WCA quickly recovered from 0° to 104°, achieving an immediate superhydrophilic-to-hydrophobic transition. After 120 s, the modified fabric surface fully returned to its initial highly hydrophobic state (Figs. 3e and 3f). Systematic testing of poly(Azo-*co*-MPTSS)-modified fabrics with different comonomer ratios showed robust, reversible light-controlled wettability switching from strong hydrophobic to superhydrophilic (Fig. 3g). All samples displayed highly consistent cyclic WCA switching under repeated alternating UV/Vis irradiation. Considering the initial hydrophobicity, azobenzene content, and film-forming ability of the coating, the poly(Azo-*co*-MPTSS) system with an Azo: MPTSS ratio of 8:1 was selected as the optimal formulation for subsequent mechanical durability and application performance characterization. Furthermore, cycle tests showed negligible attenuation of the WCA variation over 20 alternating UV/visible-light irradiation cycles, revealing outstanding photostability and reliable dynamic control of the surface wettability (Fig. 3h). Moreover, compared with previously reported smart surfaces responsive to light, gas, pH, and temperature, the present azo-copolymer-modified fabric displayed significantly faster and more distinct light-triggered wettability switching (Fig. 3i).[5,33,34,45–66]

It is well known that the mechanical robustness and chemical stability of smart fabric surfaces are critical prerequisites for their promising applications in surface science and engineering. As shown in Fig. 4(a), the azo-copolymer-modified fabric retained its high hydrophobicity with a nearly unchanged water contact angle even after a 20-cycle abrasion test under a 20 g load. The reversible light-triggered wettability transition of the abraded fabric was further investigated, revealing that the WCA could still be reversibly switched above 135° and 0°, demonstrating that the photoresponsive wettability of the azo-copolymer coating was well preserved upon mechanical abrasion (Fig. 4b). Meanwhile, the SEM images and SEM-EDS elemental mapping verified that the azo-copolymer coating remained structurally intact with a homogeneous distribution of C, O, Si, and N, confirming the stable immobilization of the copolymer on the fabric surface (Figs. 4c–4h). In addition, tape peeling adhesion tests were per-

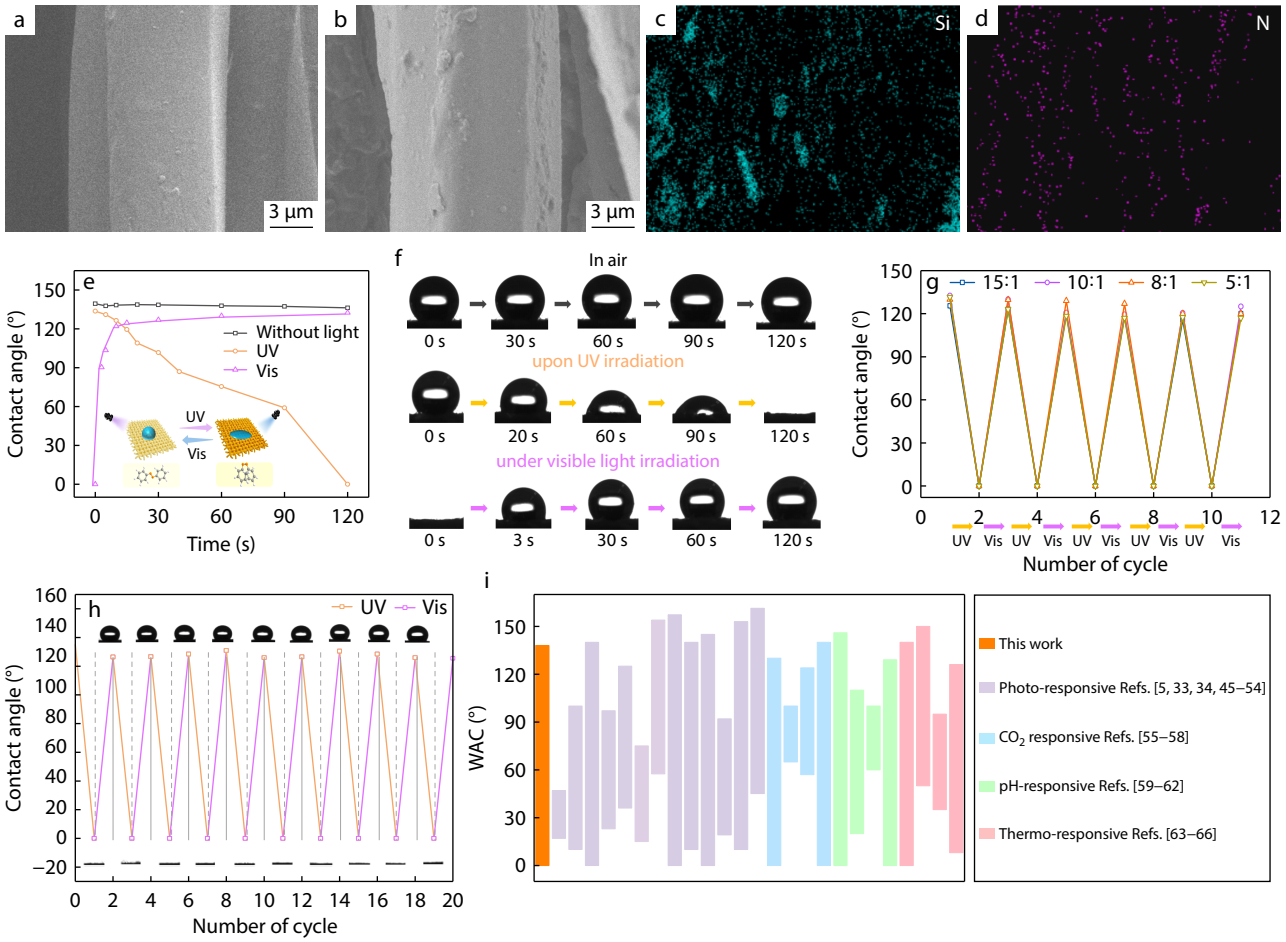

Fig. 3 SEM images of cotton fabrics (a) before and (b) after azo-copolymer modification; (c, d) Corresponding SEM-EDS elemental mappings of the modified fabric. (e) Time-dependent water contact angle (WCA) variations of fabric surfaces under ambient conditions (black line), UV irradiation (yellow line), and subsequent visible-light irradiation (purple line), with the inset illustrating light-triggered surface wettability switching. (f) Photographs of water droplets on the modified fabric at varied times. (g) Light-induced reversible WCA transitions of fabrics modified with poly(Azo-*co*-MPTSS) at different monomer molar ratios. (h) Photoresponsive wettability stability of the modified fabric; (i) Comparison of its photoresponsive wettability performance with reported work.

formed to evaluate the bonding stability between the azo-copolymer coating and the cotton fibers. No coating shedding was observed, indicating strong interfacial adhesion between the azo-copolymer and the cotton substrates (Fig. S7 in ESI). Furthermore, after cyclic curling, folding, and stretching, the pristine hydrophobic water contact angle of the modified fabric in the dark state slightly decreased. The modified fabric could stably switch to a hydrophilic state under UV irradiation, with its surface wettability reversibly restored upon visible light irradiation (Fig. 4i). To evaluate the durability against various corrosive environments, the azo-copolymer-modified fabric samples were immersed in aqueous solutions of different pH values for 24 h (Fig. 4j). Notably, after 24 h of immersion, the solutions remained visually uniform and transparent with no obvious delamination or detachment of the azo-copolymer coating (Fig. 4k). Moreover, no obvious color change was observed on the surface of the azo-copolymer-modified fabric (Fig. S8 in ESI). In addition, semi-quantitative analysis based on UV-Vis absorption spectra and transmittance measurements of the solutions before and after immersion showed no discernible changes due to azo-copolymer leaching, further confirming the excellent chemical corrosion resistance of the as-fabricated smart fabric surfaces (Figs. 4l–4n).

On the pronounced wettability transition from strong hydrophobicity to superhydrophilicity observed on azo-copolymer-modified fabric surfaces, and motivated by the convenient spatiotemporal control of light, the facile construction of visually patterned surfaces on smart fabrics was successfully achieved *via* selective UV and visible-light exposure strategies (Fig. 5). Upon selective UV irradiation, the wettability of the exposed regions switched from the original high hydrophobicity to superhydrophilicity, whereas the unexposed regions retained their initial highly hydrophobic state and repelled water droplets, enabling the formation of an optically discernible "rose" pattern (Fig. 5a → Fig. 5b). Subsequently, upon blanket UV irradiation, the entire fabric surface became superhydrophilic uniformly (Fig. 5b → Fig. 5c). Furthermore, selective visible-light illumination allowed the local restoration of superhydrophobicity, generating well-defined "peony" hydrophobic patterns on the fabric surface (Fig. 5c → Fig. 5d). Moreover, blanket exposure to visible light erases the

https://doi.org/10.1007/s10118-026-3728-0

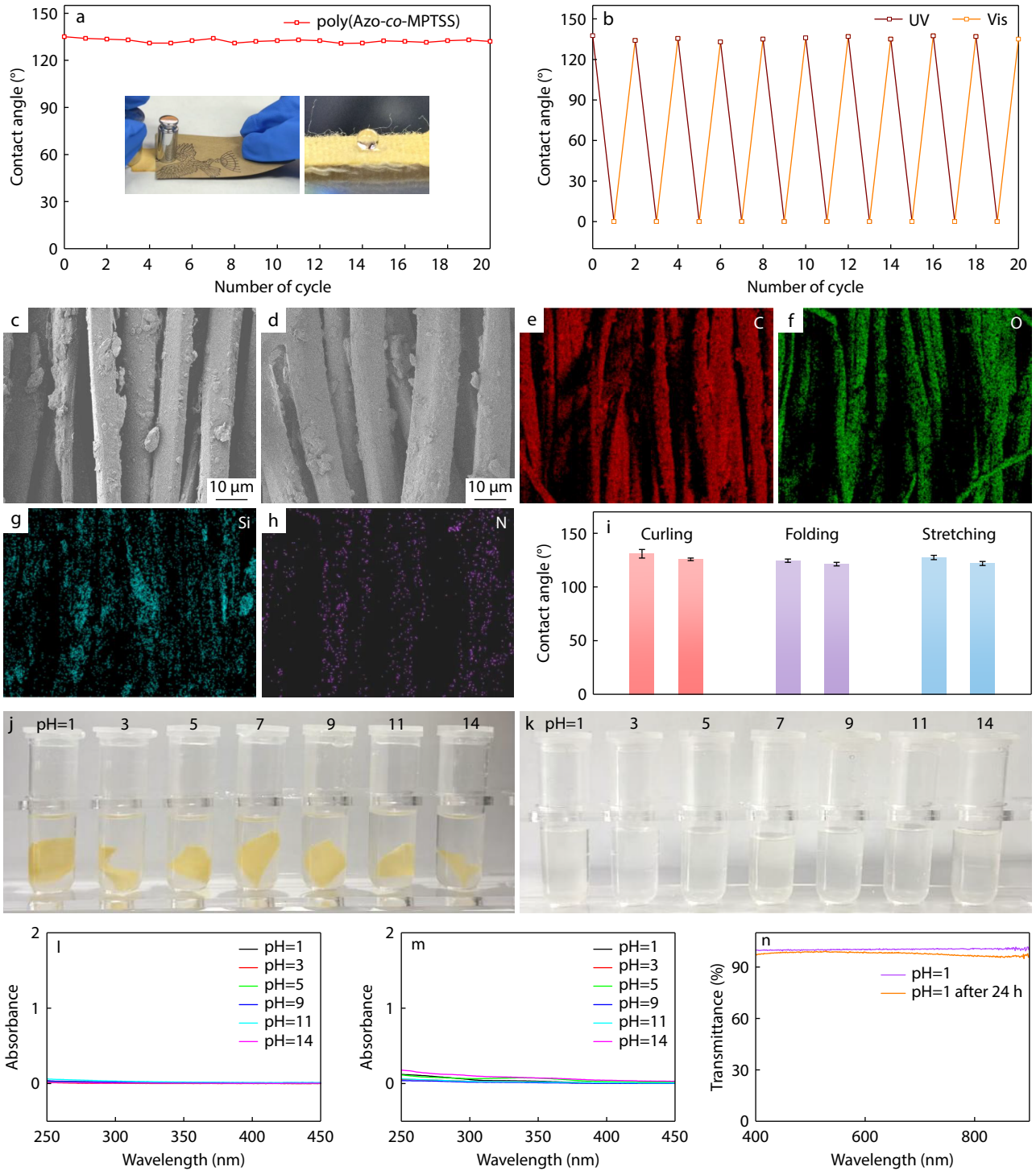

Fig. 4 (a) Abrasion resistance of the modified fabric coating; (b) Photoresponsive wettability after abrasion; SEM images of the modified fabric (c) before and (d) after abrasion, and (e–h) corresponding SEM-EDS mappings; (i) Water contact angles of modified cotton fabric under dark, UV and Vis light irradiation conditions after cyclic mechanical curling, folding and stretching treatments; Photographs of the modified fabrics immersed in different pH aqueous solutions for 24 h (j) and the corresponding solution after removal of the fabric (k); UV-Vis absorption spectra of modified fabrics before (l) and after (m) acid/alkaline solutions immersion; (n) Transmittance measurements.

"peony" pattern, restoring the fabric surface wettability to its initial state (Fig. 5d → Fig. 5a). Under ambient laboratory conditions, the visualized contrast of the formed wettability patterns was stably maintained and clearly distinguishable for over 1 h, confirming satisfactory long-term information retention. Moreover, after 30 repeated UV/Vis alternating writing-erasing cycles, the reversible switching clarity and morphological integrity of the wettability patterns exhibited negligi-

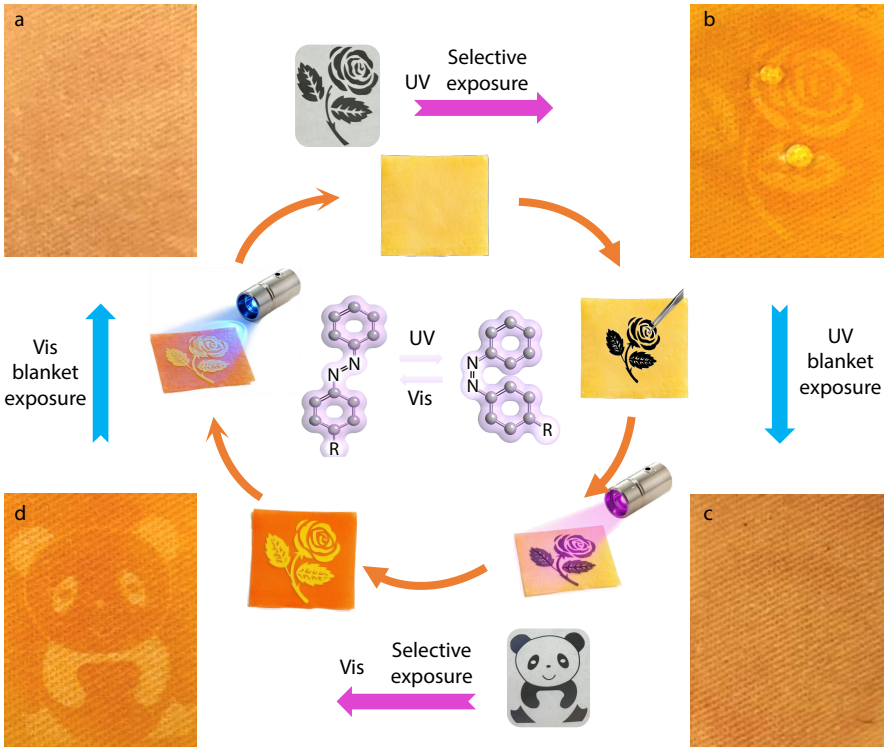

Fig. 5 Smart-fabric wettability-patterned surface construction and applications: (a) as-prepared highly hydrophobic fabric surface; (b) patterned superhydrophilic fabric surface after selective UV irradiation; (c) globally superhydrophilic fabric surface resulting from blanket UV exposure; (d) patterned highly hydrophobic fabric surface restored by selective visible-light irradiation.

ble attenuation, verifying the excellent cyclic durability and rewritability of the patterned information storage system (Figs. S9 and S10 in ESI). Therefore, by employing selective light exposure with different photomasks, diverse rewritable super-wettable patterned surfaces can be fabricated reversibly and conveniently. This high-efficiency wettability patterning approach holds great promise for potential applications in information storage, biosensors, and microreactors.[3,8,67,68]

CONCLUSIONS

In conclusion, we report a simple dip-coating strategy to fabricate cotton fabric-based, robust, photoresponsive superwetting smart surfaces using novel fluorine-free photoresponsive azo-copolymers. The reversible *trans-cis* isomerization of photoresponsive azobenzene moieties endows the smart fabric surfaces with excellent photoswitchable wettability, whereas the low-surface-energy organosilicon moieties in the azo-copolymer confer excellent initial hydrophobicity to the surface. The as-prepared smart fabrics exhibited rapid and reversible wettability switching between high hydrophobicity and superhydrophilicity under alternating UV and visible light irradiation. More importantly, smart fabric surfaces demonstrate outstanding chemical and mechanical robustness, enabling resistance to harsh environmental conditions, repeated abrasion, and various mechanical deformations. Furthermore, smart fabric surfaces provide a rewritable platform for patterning wettability *via* selective light irradiation, with promising potential for applications in information storage, biosensing, and microreactor technologies.

Conflict of Interests

The authors declare no interest conflict.

Electronic Supplementary Information

Electronic supplementary information (ESI) is available free of charge in the online version of this article at http://doi.org/10.1007/s10118-026-3728-0.

Data Availability Statement

The data supporting the findings of this study are available from the corresponding author upon reasonable request.

ACKNOWLEDGMENTS

This work was financially supported by the Natural Science Foundation of Shandong Province (Nos. ZR2022MB034 and ZR2025QC512), Key Research and Development Program of Shandong Province (No. 2024TSGC0909) and the National Natural Science Foundation of China (No. 52503154).

REFERENCES

1 Zhou, H., Niu, H., Wang, H., Lin, T. Self-healing superwetting

Graphical Abstract

Molecularly Engineered Eco-friendly Smart Fabrics with Photoswitchable Wettability: from Highly Hydrophobic to Superhydrophilic

Yiran Wang, Bo-Lun Feng, Hong-Fei Jiang, Lin Zhang, Bin Chen, Hao-Kai Yuan, Lu Wang, and Chuan-Yong Zong

University of Jinan

A fluorine-free azo-copolymer smart fabric shows reversible photoswitchable wettability from hydrophobic to superhydrophilic, with robust chemical and mechanical stability, enabling diverse, rewritable wettability patterns *via* selective light exposure.

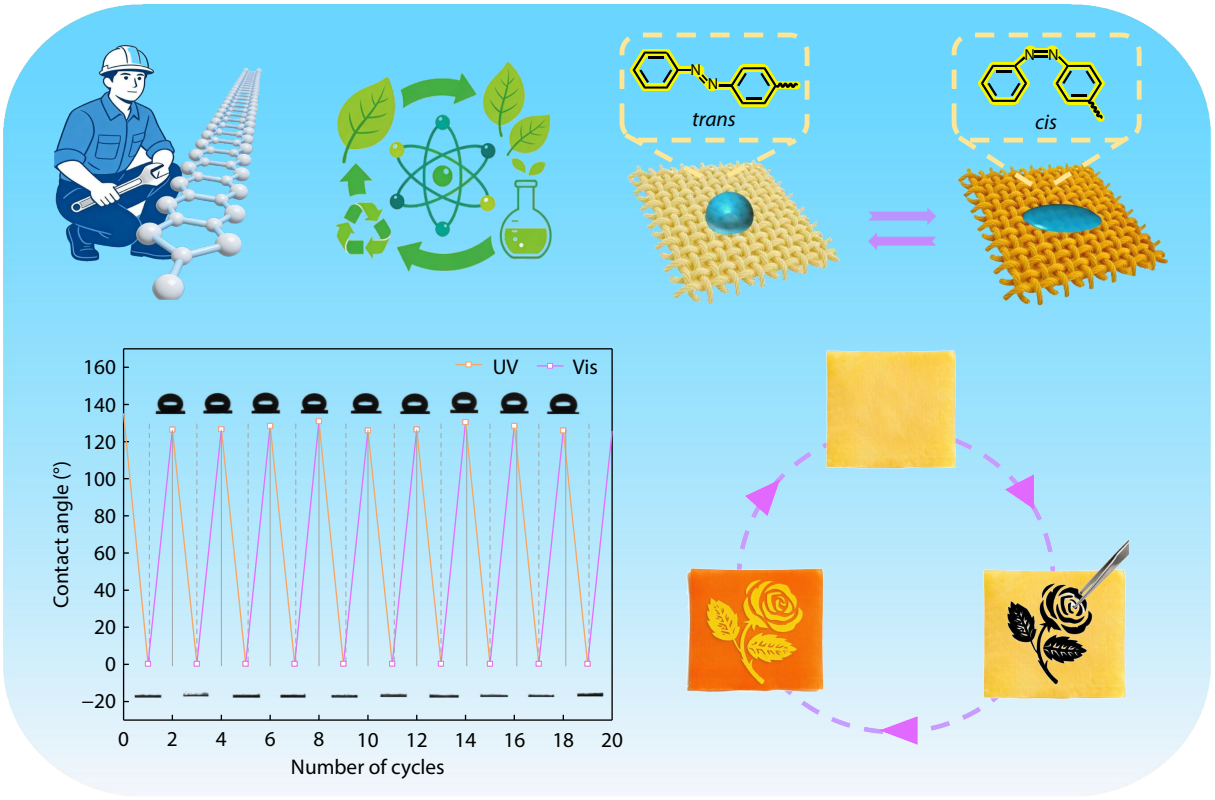

Chinese J. Polym. Sci., 2026 *https://doi.org/10.1007/s10118-026-3728-0*

surfaces, their fabrications, and properties. *Chem. Rev.* **2022**, *123*, 663−700.

2 Zhou, S., Jiang, L., Dong, Z. Overflow control for sustainable development by superwetting surface with biomimetic structure. *Chem. Rev.* **2022**, *123*, 2276−2310.

3 Shao, H., Yin, K., Xu, N., Zhang, Y., Shi, Z., Zhou, Y., Luo, Z., Wang, D., Deng, X. Adaptive surfaces with stimuli-responsive wettability: from tailoring to applications. *ACS Nano* **2025**, *19*, 6729−6747.

4 Yang, T., Wang, S., Yang, H., Gui, H., Du, Y., Liang, F. Temperature-triggered dynamic Janus fabrics for smart directional water transport. *Adv. Funct. Mater.* **2023**, *33*, 2214183.

5 Chen, J., Chen, X., Azhar, U., Yang, X., Zhou, C., Yan, M., Li, H., Zong, C. Flexible and photo-responsive superwetting surfaces based on porous materials coated with mussel-inspired azo-copolymer. *Chem. Eng. J.* **2023**, *466*, 143176.

6 Zhang, H., Wang, F., Guo, Z. The antifouling mechanism and application of bio-inspired superwetting surfaces with effective antifouling performance. *Adv. Colloid Interface Sci.* **2024**, *325*, 103097.

7 Wang, X., Liu, Y., Cheng, H., Ouyang, X. Surface wettability for skin-interfaced sensors and devices. *Adv. Funct. Mater.* **2022**, *32*, 2200260.

8 Sun, L., Guo, J., Chen, H., Zhang, D., Shang, L., Zhang, B., Zhao, Y. Tailoring materials with specific wettability in biomedical engineering. *Adv. Sci.* **2021**, *8*, 2100126.

9 Xiang, B., Sun, Q., Zhong, Q., Mu, P., Li, J. Current research situation and future prospect of superwetting smart oil/water

separation materials. *J. Mater. Chem. A* **2022**, *10*, 20190–20217.
10 Rehman, A., Sohail, M., Baig, N., Yuan, K., Abdala, A., Wahab, M.A. Next-generation stimuli-responsive smart membranes: developments in oil/water separation. *Adv. Colloid Interface Sci.* **2025**, *341*, 103487.
11 Yang, C., Zeng, Q., Huang, J., Guo, Z. Droplet manipulation on superhydrophobic surfaces based on external stimulation: a review. *Adv. Colloid Interface Sci.* **2022**, *306*, 102724.
12 Lori Zoudani, E., De Saram, P., Feih, S., Vu, H.H., Nguyen, N.T., Kashaninejad, N. Micropatterned surfaces with unidirectional wetting properties for liquid transport. *Small Struct.* **2026**, *7*, e202500492.
13 Bai, X., Gou, X., Zhang, J., Liang, J., Yang, L., Wang, S., Hou, X., Chen, F. A review of smart superwetting surfaces based on shape-memory micro/nanostructures. *Small* **2023**, *19*, 2206463.
14 Liu, X., Jia, L., Li, Y., Zhao, R., Wu, C., Xie, Z., Cheng, Z., Liu, Y., Zhang, D. Shape memory arrays top coated by adjustable mushroom with switchable adhesion to both solid and liquid. *Adv. Funct. Mater.* **2024**, *34*, 2312869.
15 Shao, Y., Du, W., Fan, Y., Zhao, J., Zhang, Z., Ren, L. Near-infrared light accurately controllable superhydrophobic surface from water sticking to repelling. *Chem. Eng. J.* **2022**, *427*, 131718.
16 Shao, Y., Wang, L., Zhu, D., Li, H., Zhang, Z., Ren, L. Photo/thermal/magnetic triple-stimuli-responsive bioinspired intelligent surface for cross-species functional regulation. *Chem. Eng. J.* **2026**, *531*, 173978.
17 Zhou, Y., Yang, G., Wang, Y., Lei, J., Ye, T., Huang, R., Zhan, S., Tang, D. Coordination-driven self-assembly of PNIPAM on MnO2 microflowers/CFC membrane with switchable superwettability for robust photo and thermal dual-responsive oil-water separation. *Compos. Part B* **2025**, *307*, 112862.
18 Chen, C., Huang, Z., Zhu, S., Liu, B., Li, J., Hu, Y., Wu, D., Chu, J. In situ electric-induced switchable transparency and wettability on laser-ablated bioinspired paraffin-impregnated slippery surfaces. *Adv. Sci.* **2021**, *8*, 2100701.
19 Wang, J., Zhu, Z., Liu, P., Yi, S., Peng, L., Yang, Z., Tian, X., Jiang, L. Magneto-responsive shutter for on-demand droplet manipulation. *Adv. Sci.* **2021**, *8*, 2103182.
20 Zhan, Y., Yu, S., Amirfazli, A., Siddiqui, A.R., Li, W. Magnetically responsive superhydrophobic surfaces for microdroplet manipulation. *Adv. Mater. Interfaces* **2022**, *9*, 2102010.
21 Rao, Q., Tong, Z., Song, L., Ali, A., Hou, Y., He, Q., Lu, J., Gao, X., Zhan, X., Zhang, Q. NIR-driven fast construction of patterned-wettability on slippery lubricant infused surface for droplet manipulation. *Chem. Eng. J.* **2022**, *428*, 131141.
22 Long, J., Liu, S., Li, N., Yuan, G., Liu, Y., Huang, Q., Li, J., Zhang, H., Wang, M. Smart surfaces with pH-responsiveness enhanced by multiscale hierarchical structures fabricated by laser direct writing. *ACS Appl. Mater. Interfaces* **2023**, *15*, 56490–56499.
23 Gan, S., Li, H., Zhu, X., Liu, X., Wei, K., Zhu, L., Wei, B., Luo, X., Zhang, J., Xue, Q. Constructing scalable membrane with tunable wettability by electrolysis-induced interface pH for oil-water separation. *Adv. Funct. Mater.* **2023**, *33*, 2305975.
24 Chen, S., Li, L., Feng, M., Huang, T., Zhang, N., Wang, Y. UV-activated superwetting ability of electrospun polysulfone/titanium dioxide membranes toward highly efficient methylene blue removal and oil/water separation. *J. Membr. Sci.* **2024**, *695*, 122450.
25 Lv, Z., Yang, Y., Zhang, L., Feng, P., Zhai, X., Zhou, C. Reversible conversion superwetting coatings with TiO_2-based heterojunction materials for enhancing efficient oily water treatment and water purification. *J. Hazard. Mater.* **2025**, *497*, 139689.
26 Fu, S., Zhou, Y., Zhao, J., Pei, K., Guo, Z. Emerging light-responsive functional surfaces for droplet manipulation. *Appl. Mater. Today* **2024**, *40*, 102429.
27 Lim, H. S., Kwak, D., Lee, D. Y., Lee, S. G., Cho, K. UV-driven reversible switching of a roselike vanadium oxide film between superhydrophobicity and superhydrophilicity. *J. Am. Chem. Soc.* **2007**, *129*, 4128–4129.
28 Zong, C., Hu, M., Azhar, U., Chen, X., Zhang, Y., Zhang, S., Lu, C. Smart copolymer-functionalized flexible surfaces with photoswitchable wettability: From superhydrophobicity with "rose petal" effect to superhydrophilicity. *ACS Appl. Mater. Interfaces* **2019**, *11*, 25436–25444.
29 Wang, N., Wang, H., Wang, K., Zuo, J., Wang, Z. Reversible dual stimuli-responsive polymer coatings with antimicrobial properties for oil-water separation. *J. Water Process Eng.* **2025**, *77*, 108484.
30 Nezhadghaffar-Borhani, E., Abdollahi, A., Roghani-Mamaqani, H., Salami-Kalajahi, M. Photoswitchable surface wettability of ultrahydrophobic nanofibrous coatings composed of spiropyran-acrylic copolymers. *J. Colloid Interface Sci.* **2021**, *593*, 67–78.
31 Li, C., Zhang, C., Zhao, R., Zhao, N., Liu, R., Zhang, Y., Jia, M., Wang, S. Porous electrospun films with reversible photoresponsive microenvironmental humidity regulation: a controllable hydrogen-bonding synergistic effect exhibited by acrylic acid segments. *ACS Appl. Mater. Interfaces* **2023**, *15*, 6187–6201.
32 Ichimura, K., Oh, S. K., Nakagawa, M. Light-driven motion of liquids on a photoresponsive surface. *Science* **2000**, *288*, 1624–1626.
33 Zhang, Z., Chen, D., Mutruc, D., Hecht, S., Heinke, L. Optical and chemical control of the wettability of nanoporous photoswitchable films. *Chem. Commun.* **2022**, *58*, 13963–13966.
34 Manabe, K., Saito, K., Nakano, M., Ohzono, T., Norikane, Y. Light-driven liquid conveyors: Manipulating liquid mobility and transporting solids on demand. *ACS Nano* **2022**, *16*, 16353–16362.
35 Herrera, J.M., Penoff, M.E., Galante, M.J. Reversible photo-controllable surface wettability of epoxy-polyurethane smart coating. *Prog. Org. Coat.* **2023**, *179*, 107509.
36 Feng, B., Zhai, C., Zhang, D., Guo, H., Zhang, H., Zhang, L., Li, H., Wang, L., Lei, L., Zong, C. Robust photo-responsive superwetting surfaces on hierarchical-structured copper mesh via dip-coating with mussel-inspired azo-copolymer. *Chinese J. Polym. Sci.* **2025**, *43*, 1134–1145.
37 Pafiti, K.S., Loizou, E., Patrickios, C.S., Porcar, L. End-Linked semifluorinated amphiphilic polymer conetworks: Synthesis by sequential reversible addition-fragmentation chain transfer polymerization and characterization. *Macromolecules* **2010**, *43*, 5195–5204.
38 Wang, T., Yang, J., Cao, Q., Pu, X., Li, Y., Chen, H., Zhao, J., Zhang, Y., Chen, X., Li, X. Room temperature nondestructive encapsulation *via* self-crosslinked fluorosilicone polymer enables damp heat-stable sustainable perovskite solar cells. *Nat. Commun.* **2023**, *14*, 1342.
39 Hartley, G.S. The cis-form of azobenzene. *Nature* **1937**, *140*, 281–281.
40 Zong, C., Zhao, Y., Ji, H., Han, X., Xie, J., Wang, J., Cao, Y., Jiang, S., Lu, C. Tuning and erasing surface wrinkles by reversible visible-light-induced photoisomerization. *Angew. Chem. Int. Ed.* **2016**, *55*, 3931–3935.
41 Bandara, H.D., Burdette, S.C. Photoisomerization in different classes of azobenzene. *Chem. Soc. Rev.* **2012**, *41*, 1809–1825.
42 Kumar, G., Neckers, D. Photochemistry of azobenzene-containing polymers. *Chem. Rev.* **1989**, *89*, 1915–1925.
43 Zhang, P., Lan, Z., Wei, J., Yu, Y. Photodeformable azobenzene-containing polyimide with flexible linkers and molecular alignment. *ACS Macro Lett.* **2021**, *10*, 469–475.
44 Zhou, C., Zhao, X., Zhao, X., Li, H., Zhang, S., Feng, W., Zhang, Y.

Low ice adhesion surfaces based on flexible fluorinated polymers with a polynorbornene backbone. *ACS Appl. Mater. Interfaces* **2020**, *12*, 53494−53502.
45 Babazadeh-Mamaqani, M., Roghani-Mamaqani, H., Rezaei, M., Salami-Kalajahi, M. Photo-induced time-dependent controllable wettability of dual-responsive multi-functional electrospun MXene/polymer fibers. *J. Colloid Interface Sci.* **2025**, *678*, 1048−1063.
46 Kang, H., Liu, Y., Lai, H., Yu, X., Cheng, Z., Jiang, L. Under-oil switchable superhydrophobicity to superhydrophilicity transition on TiO_2 nanotube arrays. *ACS Nano* **2018**, *12*, 1074−1082.
47 Yang, D., Zeng, Q., Tan, K., Hou, H., Fang, X., Guo, C., Yuan, H., Meng, T. Lipase-entrapped colloidosomes with light-responsive wettability for efficient and recyclable Pickering interfacial biocatalysis. *Green Chem.* **2024**, *26*, 10824−10828.
48 Domalanta, M. R. B., Ali, M. R. R., Maalihan, R. D., Caldona, E. B. Photo-and thermoresponsive reversible wettability and corrosion protection of electrophoretically deposited TiO_2/Pectin composite coatings. *Langmuir* **2025**, *41*, 11958−11967.
49 Gao, H. P., Chang, S. Y., Liu, Y., Meng, Z., Han, Z. W., Ren, L. Q. Interlaced wetting surfaces with switchable wettability for manipulating underwater oil droplets. *Chem. Eng. J.* **2022**, *437*, 135007.
50 Juan, L., Chenxi, Y., Ziru, N., Shenglan, Y., Dongwen, H. Fabrication of flexible photo-responsive mesh with reversible wettability and enhanced mechanical damage resistance for efficient oil/ water separation. *J. Environ. Chem. Eng.* **2024**, *12*, 114857.
51 Shen, J., Yuan, Y.Z., Yu, H.M., Tian, X.H., Zhang, Y. Smart wood membrane with reversible photo-responsive wettability for intelligent oil-water separation. *Chem. Eng. J.* **2026**, *531*, 173904.
52 Hu, W.H., Huang, J.G., Zhang, X., Zhao, S.P., Pei, L., Zhang, C.Y., Liu, Y.Q., Wang, Z. A mechanically robust and reversibly wettable benzoxazine/epoxy/mesoporous TiO_2 coating for oil/water separation. *Appl. Surf. Sci.* **2020**, *507*, 145168.
53 Li, Y.L., Shi, B.Y., Luan, X.Y., Hao, Z.H., Wang, Y.F. Achieving reversible superhydrophobic-superhydrophilic switching of lignocellulosic paper surface with modified nano-TiO_2 coating. *Polym. Test.* **2022**, *116*, 107789.
54 Yao, F., Wei, J., Xu, Y.J., Tu, H., Huang, M., Tang, Q.F., Zhao, S., Wang, J. Light-trapping superhydrophobic coatings with switchable wettability to solve low-temperature anti-icing/deicing and high-temperature overheating problems on surfaces. *J. Colloid Interface Sci.* **2025**, *699*, 138275.
55 Abraham, S., Kumaran, S.K., Montemagno, C.D. Gas-switchable carbon nanotube/polymer hybrid membrane for separation of oil-in-water emulsions. *RSC Adv.* **2017**, *7*, 39465−39470.
56 Yin, H., Zhan, F., Li, Z., Huang, H., Marcasuzaa, P., Luo, X., Feng, Y., Billon, L. CO_2-Triggered ON/OFF wettability switching on bioinspired polylactic acid porous films for controllable bioadhesion. *Biomacromolecules* **2021**, *22*, 1721−1729.
57 Qi, Z., Liu, Y., Gao, Q., Tao, D., Wang, Y., Guo, J., Yu, Y. CO_2-responsive nanofibrous membranes with gas-tunable wettability for switchable oil/water separation. *React. Funct. Polym.* **2023**, *182*, 105481.
58 Li, X., Liu, J., Qu, R., Zhang, W., Liu, Y., Zhai, H., Wei, Y., Hu, H., Feng, L. Universal and tunable liquid-liquid separation by nanoparticle-embedded gating membranes based on a self-defined interfacial parameter. *Nat. Commun.* **2021**, *12*, 80.
59 Li, L., Rong, L., Xu, Z., Wang, B., Feng, X., Mao, Z., Xu, H., Yuan, J., Liu, S., Sui, X. Cellulosic sponges with pH responsive wettability for efficient oil-water separation. *Carbohydr. Polym.* **2020**, *237*, 116133.
60 Qian, C., Li, F., Qu, J., Guo, J., Liu, J., Yang, L. The fabrication and research of pH-responsive cement-based materials with switchable wettability. *J. Build. Eng.* **2024**, *94*, 109946.
61 Choi, E., Byun, S., Jeong, S. Fabrication and evaluation of pH-sensitive chitosan-coated membranes for enhanced oil emulsion filtration. *Membranes* **2025**, *15*, 252.
62 Song, Y., Zhang, L., Dong, L., Li, H., Yu, Z., Liu, Y., Lv, G., Ma, H. pH-responsive smart wettability surface with dual bactericidal and releasing properties. *ACS Appl. Mater. Interfaces* **2021,** *13*, 46065-46075.
63 Zhang, W., Liu, N., Zhang, Q., Qu, R., Liu, Y., Li, X., Wei, Y., Feng, L., Jiang, L. Thermo-driven controllable emulsion separation by a polymer-decorated membrane with switchable wettability. *Angew. Chem. Int. Ed.* **2018**, *57*, 5740−5745.
64 Banuprasad, T.N., Vinay, T.V., Subash, C.K., Varghese, S., George, S.D., Varanakkottu, S.N. Fast transport of water droplets over a thermo-switchable surface using rewritable wettability gradient. *ACS Appl. Mater. Interfaces* **2017**, *9*, 28046−28054.
65 Marri, G.K., Kumar, N., Sett, S. Phase-variant lubricant-infused surfaces with thermoresponsive wettability switching. *ACS Mater. Lett.* **2025**, *7*, 3537−3544.
66 Dou, J., Ma, L., Lin, S., Lu, J., Zhang, C., Li, Z., Jiang, H., Shi, G., Cui, Y., Zhang, L. Thermo-responsive reverse osmosis membranes with switchable wettability for enhanced antifouling and self-cleaning performance. *J. Membr. Sci.* **2026**, *741*, 125034.
67 Wang, Y., Sun, Y., Xue, Y., Sui, X., Yuan, B., Wang, Y., Liang, W. Functional surfaces with reversibly switchable wettability: Fundamentals, progresses, applications and challenges. *Prog. Org. Coat.* **2024**, *188*, 108167.
68 Cai, Y., Cui, Q.Y., Zhang, H.R., Ma, X.L., Xue, M.Q. Promoted non-enzymatic glucose sensor based on synergistic effect of hydrothermal synthesized $Ni(OH)_2$-graphene Nanocomposite. *Chem. Res. Chin. Univ.* **2024**, *40*, 914−921.